



Feedback-based positioning and diffusion suppression of particles via optical control of thermoviscous flows

ELENA ERBEN,^{1,2} BENJAMIN SEELBINDER,^{1,2} ILIYA D. STOEV,^{1,2}
SERGEI KLYKOV,^{1,2} NICOLA MAGHELLI,^{1,2} AND MORITZ
KREYSING^{1,2,3,*}

¹Max Planck Institute of Molecular Cell Biology and Genetics, Pfotenhauerstraße 108, 01307 Dresden, Germany

²Center for Systems Biology, Pfotenhauerstraße 108, 01307 Dresden, Germany

³Cluster of Excellence Physics of Life, TU Dresden, Dresden, Germany

*kreysing@mpi-cbg.de

Abstract: The ability to control the position of micron-size particles with high precision using tools such as optical tweezers has led to major advances in fields such as biology, physics and material science. In this paper, we present a novel optical strategy to confine particles in solution with high spatial control using feedback-controlled thermoviscous flows. We show that this technique allows micron-size particles to be positioned and confined with subdiffraction precision (24 nm), effectively suppressing their diffusion. Due to its physical characteristics, our approach might be particularly attractive where laser exposure is of concern or materials are inherently incompatible with optical tweezing since it does not rely on contrast in the refractive index.

© 2021 Optical Society of America under the terms of the [OSA Open Access Publishing Agreement](#)

1. Introduction

The manipulation of micron-size particles, particularly their high-precision positioning, remains an active research topic with applications in the life sciences, engineering and manufacturing. Examples of successfully used technologies include optical [1–4], magnetic [5–7], electrokinetic [8,9], acoustic [10] and thermophoretic trapping [11], the positioning of self-propelled Janus particles [12] and gas bubbles [13]. However, some of these techniques require specific material properties of the particles or the environment in which they can be applied. To overcome this constraint, hydrodynamic trapping has been successfully deployed, and is particularly attractive for the life sciences, but currently lacks optical control. Current hydrodynamic trapping methods can be subdivided into contact-based methods [14,15], where dissolved particles are immobilized against walls, wells, posts or other obstacles by fluid flow, and non-contact methods, where particles can be confined in stagnation-point flows [16,17], microvortices [18] or microeddies [19]. Active feedback control of flows in multi-inlet chambers has been demonstrated to control the position of stagnation-point flows and allows users to manipulate the particle position and counteract particle displacements due to diffusion [16,17]. With this method, it is feasible to control the position of single colloidal particles with a precision of 78 nm [17].

Although current hydrodynamic trapping methods pose reduced constraints on the material properties of the trapped particle [20], high-precision manipulation of particles requires the use of extremely precise and stable microfluidic pumps. Furthermore, hydrodynamic trapping by definition requires special chambers and cannot be used to generate flows in closed systems such as a cell. Additionally, the generated flows are global, typically ranging between pumps and outlets, which renders the spatial resolution of this technique way lower than many optical technologies.

Another way to position particles with high precision could be to make use of thermoviscous flows, which can be optically controlled. These have been described as the directed motion of aqueous media in response to travelling temperature fields [21], an emergent physical phenomenon driven by the thermal expansion of fluids in non-homogenous viscosity fields (compare Fig. 1(b)). In particular, thermoviscous flows have been used to transport aqueous solutions visualized by tracer particles or molecules along an optically defined path [21,22]. More recently, we showed that these flows can also be induced in cells and developing embryos [23–25], where they give rise to a streaming of the cytoplasm, albeit with limited abilities to control the positioning of colloids immersed in the cytoplasm. However, it has yet to be shown whether optically generated thermoviscous flows could be used to enable the precise positioning of a pre-specified object or whether such positioning could be automated.

Here we show that high-precision hydrodynamic positioning of particles can be achieved all-optically by combining laser-induced thermoviscous flows with a closed feedback loop that takes into account the time-dependent and stochastic particle positions. We analyze the physical characteristics of this novel way to control particle position. While optically facilitated, we achieve a precision of up to 24 nm, which is unprecedented by classic hydrodynamic trapping and only slightly above the localization accuracy (with a mean value of 9.5 nm in these experiments, see Supplement 1, Fig. S3). In contrast to optical tweezers, our method requires neither specific materials nor the exposure of particles to the laser beam. We conclude that optically induced feedback-controlled thermoviscous flows are an attractive alternative to classic hydrodynamic trapping techniques, while generating opportunities for a wide range of novel applications.

2. Results

2.1. Design of optical setup & closed-loop feedback control

The experimental setup, a fluorescence optical microscope complemented by 1455 nm laser scanning optics, has been described in detail previously [23]. In brief, it comprises a continuous-wave 1455 nm Raman laser (CRFL-20-1455-OM1, 20 W, near TEM₀₀ mode profile, Keopsys) emitting a collimated laser beam that is acousto-optically deflected (AA.DTSXY-A6-145, Pegasus Optik). The deflection point is imaged into the underfilled back focal plane of a 60x 1.2NA immersion objective ($\times 60$ UPLSAPO, NA = 1.2, W-IR coating, Olympus) in an inverted fluorescence microscope (Olympus IX83), such that the LabVIEW (National Instruments) controlled deflection translates into the motion of the laser focus (diameter = 3.8 μm) inside the sample chamber, with a scanning range of approximately 150 μm .

To achieve automated positioning of beads via optically induced thermoviscous flow fields (see Fig. 1 for concept), we introduced a closed-loop feedback control. Implemented as a LabVIEW-based program, this loop repeats at around 50 Hz while consisting of 4 sequential steps (Fig. 1(c)): i) A fluorescent image of the sample (typically fluorescent beads in glycerol-water solution 50% v/v, see below) is acquired. ii) The centroid of these particles is determined using a standard routine based on thresholding segmentation and subsequent calculation of the center of mass. iii) The particle closest to the predefined destination is selected, and a laser scan path parameterized.

This scan path is parallel to the connecting vector between destination and current bead position, and is either centered on the particle (results presented in Fig. 3) or ending slightly before it (Fig. 4). iv) The laser scan is applied along the path, with a typical scan rate of 1-3 kHz, which is sufficiently slow to allow for the relaxation of temperature fields between successive scan periods.

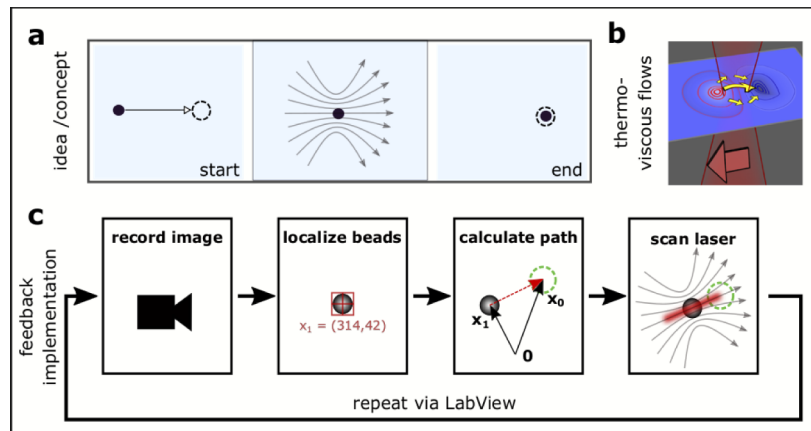


Fig. 1. Concept and implementation: Positioning of colloidal particles via optically induced thermoviscous flows. a) Concept: This work establishes the 2D precision positioning of colloidal particles via optically inducible thermoviscous flow fields. b) Thermoviscous flows are known to arise from the scanning of an infra-red laser beam through an aqueous medium by the complex interplay of thermal expansion and temperature-induced viscosity changes. c) Schematic of closed feedback loop operation to automatically position particles.

2.2. Sample preparation and specifications

Bead-positioning experiments were conducted with fluorescent beads of $3.06\ \mu\text{m}$ mean diameter (Fluoresbrite YG Microspheres $3.00\ \mu\text{m}$, 17155-2, Polysciences, USA) contained in a mixture of glycerol and water in equal parts (50% v/v) and 0.2% Tween 80 to prevent bead adhesion to surfaces. To keep the particles confined to the focal plane and achieve a uniform chamber height, spacer beads of $5.15\ \mu\text{m}$ mean diameter (PS & P(S/DVB) Polymer Particles, PS06N, Bangs Laboratories, Inc., USA) were added to the solution at a low concentration. The solution containing the beads was then sandwiched between two glass slides, sealed with dental impression material (Identium Light Fast, Kettenbach GmbH & co. KG, Germany). The chamber height was further limited through the amount of solution placed between the slides ($2\ \mu\text{L}$ solution for a $5\ \mu\text{m}$ high chamber with a cover glass diameter of $22\ \text{mm}$). To accurately determine the chamber height via confocal microscopy, some chambers additionally contained trace amounts of fluorescent particles of $0.11\ \mu\text{m}$ mean diameter (Fluorescent Carboxyl Polymer Particles (Green), FC02F, Bangs Laboratories, Inc., USA). All experiments have been carried out at room temperature.

2.3. Flow field imaging and characterization

While classic microfluidics is controlled via quasi-infinite extended flow fields, thermoviscous flows can be induced optically and locally.

To determine the localization and scaling of thermoviscous flows, which may impact both the precision of this optical manipulation and the ability to push particles while avoiding direct laser exposure, we characterized the flows as a function of distance from the laser scan path.

To accurately quantify flow velocities over distance, one needs to disentangle the lateral flow profile and a modulation along the optical axis. In thin chambers, with a height less than the circumference of a moving heat spot, it has been described that thermoviscous flows yield a response equivalent to that of a force monopole, with the momentum balance being accounted for solely by interaction with the chamber [22]. In thicker chambers with more precise focusing, such as in the setup described here, this is not necessarily the case, as counterforces might also be transferred from the lateral sides of the heat spot and onto the medium. Therefore, we set out

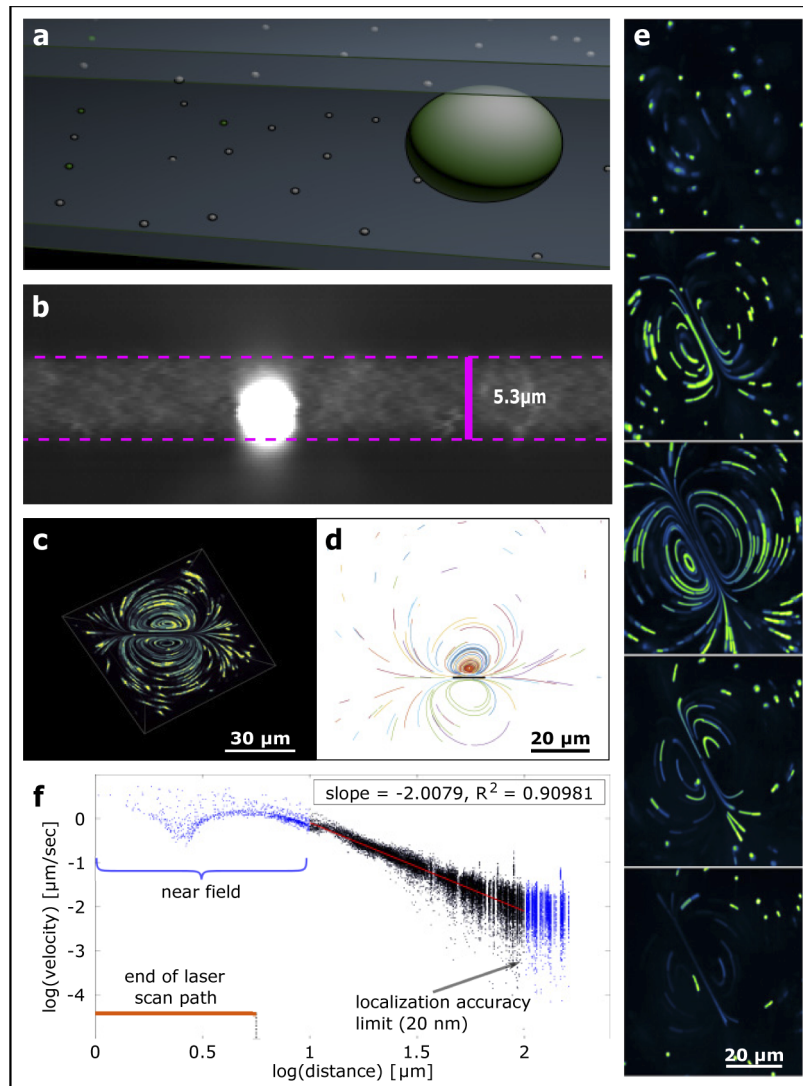


Fig. 2. Characterization of experimental chambers and optically induced flow fields via 3D confocal microscopy. a) Schematic representation of chamber design with small beads marking the surfaces and a large bead to be manipulated. b) x,z confocal section of a 5.3 μm high chamber shown as a maximum intensity projection over the out-of-plane y-dimension. c) Example of 3D confocal mapping of flow field, captured in a 25 μm high chamber with fluorescent beads of 0.5 μm diameter. See also [Visualization 1](#). d) Detected tracks of fluorescent beads moving in the flow field of an infra-red laser scan along a circa 11 μm long line (indicated in black) captured over 100 s. e) Maximum intensity projection over time showing flow field captured at different heights in the chamber, beginning and ending close to the chamber walls. f) Velocity scaling with distance from the scan center, indicating a $1/r^2$ decay at long distances. Velocity analysis from data in d.

to image flow fields in response to a 10 μm laser scan volumetrically via tracer beads and a 3D sectioning spinning disc confocal microscope (CSU-X1, Yokogawa). In addition to the in-plane modulation described before, these data show a strong modulation of the flows along the optical axis (Fig. 2(e)), with non-slip boundary conditions at the top and bottom of the chamber. Our data furthermore allow us to select images collected at the mid-plane, separating the in-plane velocity distribution and its modulation along the optical axis. This height discrimination enables an accurate quantification of flow velocities with distance. Repeating these experiments in a chamber with a highly viscous sucrose solution enabled us to track beads with a frame-to-frame reproducibility of 10 - 20 nm, accounting for both diffusive displacements and centroid tracking accuracy. As a result of this quantification, we find that experimentally determined flow fields are nearly constant in the range of the laser scan, but also extend well beyond, with flow displacements detectable as far as 100 μm away. The scaling of the flow field with radial distance in the far field shows a power law scaling with an exponent of -2.01 , $R^2 = 0.91$ (compare Fig. 2(f)). This far field closely reflects the description of sink source dipoles but also matches the characteristics of a force dipole [21], which in between two parallel plates would show scaling exponents of -2 . Higher-order contributions that account for the more complex near field are known to decay faster and will therefore not be visible in the far field.

Given a significant extension of the flow field beyond the finite-length laser scan path (compare Fig. 2(f)), our data suggest that it is feasible to position particles at a distance and without directly exposing them to the laser beam.

2.4. Guided directed motion

Starting our positioning experiments, we first tested if the setup described above could be used to guide a single fluorescent polystyrene particle to a desired position using non-stationary and co-translating optically induced flow fields. We found that using a laser scan path of approximately 10 μm length, centered on the particle, and generating a flow field locally pointing to the particle's destination suffices to iteratively move a bead to its target position (compare Fig. 3(a)). In particular, we found that the distance between particle and target decreased linearly (Fig. 3(b)) with time and with a nearly constant velocity of $-0.284 \mu\text{m/s}$. The fact that the particle moves at a constant velocity is to be understood as a direct result of the laser scan path being constantly position adjusted to remain centered on the particle (using a feedback loop that updates at a rate of approximately 50 Hz). To ensure reproducible positioning, the system would also need to adapt to displacements occurring on the trajectory of the particle. Therefore, we repeated this experiment multiple times by alternating periods of the laser being switched on and off. As a result, we observed that the particle diffusively moved away from the target when no thermoviscous flows were applied (Laser switched off) and re-approached the target as soon as the laser was switched on again (compare Fig. 3(c)). Taken together, these results suggest that the combination of optically generated thermoviscous flows with the logic of closed-loop feedback control that has previously been pioneered in advanced microfluidics is indeed capable of positioning small particles with high precision.

2.5. Feedback-based particle confinement

To determine whether a particle can be held in a pre-defined position, and to obtain better statistics on the precision of this optically controlled manipulation, we analyzed the continuous, feedback-controlled motion of the same fluorescent bead after reaching its destination. We found that the particle is effectively prevented from diffusing away by our feedback algorithm. Plotting a histogram of the position of a bead held at the target position over a time span of just over 1 min (Fig. 3(d)) revealed a near Gaussian probability-density function for the particle position with a standard deviation as low as 39.4 nm. As an important control, we observed significant diffusional displacements when repeatably pausing the flows, which showed that the particle

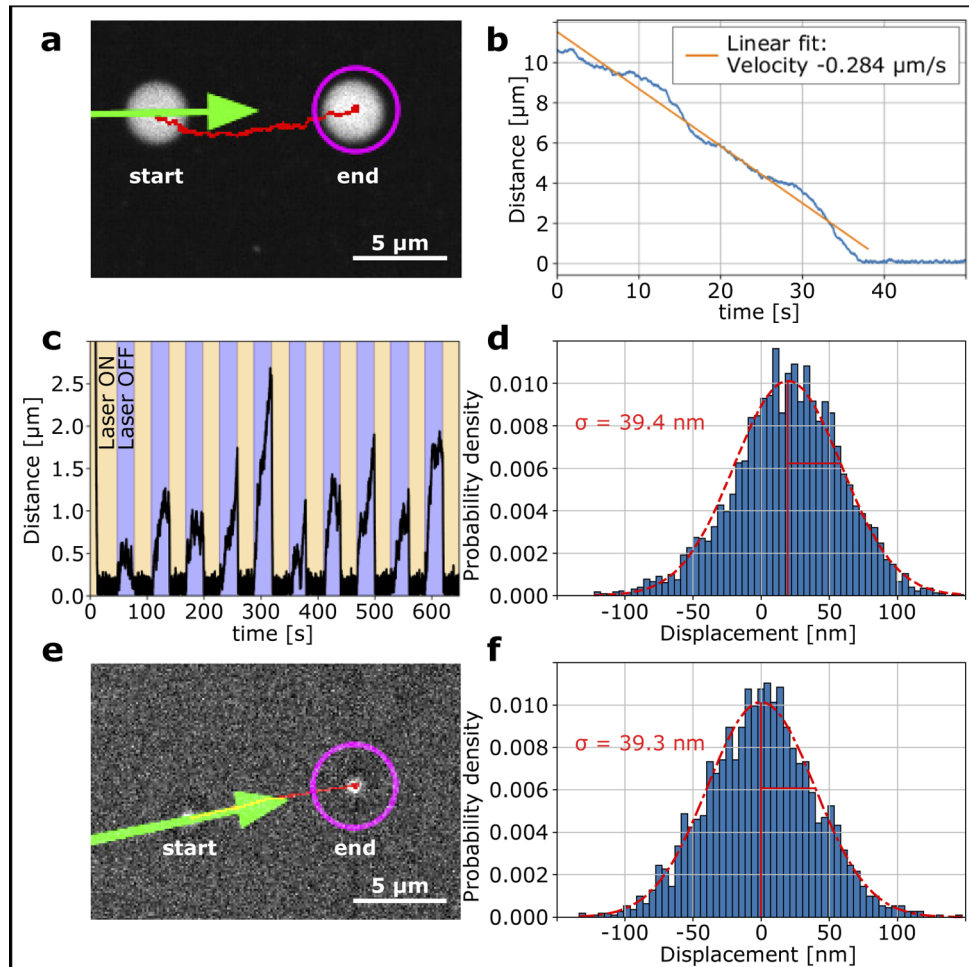


Fig. 3. Feedback based positioning of beads with positive and negative refractive index contrast via optically induced flow fields centered on the particles. a) Positioning of a polystyrene bead in a low refractive index environment (50% v/v glycerol water solution). See also [Visualization 2](#). b) Distance between the particle and the target over time. c) Distance between the particle and the target over time for alternating periods of the laser being turned on and off. d) Histogram of particle displacement from the target position; data collected over 1 min. e) Positioning of a silica bead in a high refractive index environment (pure glycerol) after re-optimization of parameters (see also [Visualization 3](#)). f) Histogram of silica bead displacement, data collected over 2 min.

did not adhere to the surface. Thus, our system not only allows for manipulating particles but can also be used to confine particles near pre-specified positions for extended periods of time, suppressing diffusion as well as possible instrument drifts.

Next we sought to rule out that optical forces could have a contribution to the confinement. Towards this end we repeated the same experiment with a particle of reduced refractive index compared to its surrounding. Specifically, we immersed 1.86 μm silica beads (SiO₂MS-2.0 1.86 μm , refractive index = 1.45, obtained by personal communication, Cospheric LLC, USA) in pure glycerol with a refractive index of 1.47. As a result we find that the motion characteristic of this bead is nearly identical (after re-optimization of laser power). Not only do we observe the directed transport to the target (Fig. 3(e)), but also the confinement shows the same efficiency (Fig. 3(f)). These results rule out that optical trapping rather than repositioning by flows is the cause for the observed confinement.

Moreover, these experiments demonstrate that the positioning of colloids is less constraint in the material choice than optical tweezers, as a high refractive index of the particle is not required.

2.6. Contact-free & subdiffraction positioning

To exclude the possibility that our findings are based on thermophoretic motion away from the heating laser beam, we repeated the above experiments of feedback-driven continuous particle positioning under different conditions and over extended periods of time. For this we i) manipulated the particle from a distance with 5 μm in between the end of the laser scan path and the particle, and ii) we compared pushing and pulling flow stimuli (see Fig. 4(a) and (b)). As expected from the analysis of flow fields, we found that the particle can also be confined with moderate spacing between laser path and particle, which again excludes the possibility that the observed confinement of the particle at the target position is due to optical forces. Moreover, despite manipulation from a distance, confinement was still very high and near identical in both modes of operation. No matter if we push the bead towards its destination or if we use the flow field from the other side to pull on the particle, we see the particle to be confined with a near identical standard deviation of 79.4 nm and 82.8 nm, respectively. We observed similar behavior across a wide range of independent experimental parameters. Specifically, we varied scan frequency, laser power, laser update rate, distance between laser scan path and particle, and length of the laser scan path (data not shown).

A particularly interesting feature of thermoviscous flows is the fact that their magnitude does not depend on the absolute viscosity of the fluid and they can be induced in highly viscous media, even including viscous honey, which would be challenging to handle with classic microfluidic pumps. As diffusion shows an inverse linear relationship with the viscosity of the environment, we asked if we could increase confinement precision even further. We found that the precision of positioning in a 70% v/v glycerol-water mixture or viscous honey can be increased up to 24.3 nm (Supplement 1, Fig. S1). Surface adhesion was ruled out by the successful flow displacement before and after the experiment. Taken together, these data clearly show that flows rather than optical trapping or thermophoresis are the cause of the subdiffraction particle confinement, while also demonstrating that manipulations can be performed at a distance.

2.7. Motion characteristics of diffusing particles

To further examine how the feedback-controlled positioning of a particle leads to an effective suppression of its diffusion, we looked at how the diffusion changes its temporal scaling when feedback flows are applied and whether suppression of diffusion can also be observed in the power spectrum of a particle. To this end, we compared the diffusive mean squared displacement (MSD) of a particle in the presence and absence of re-positioning flows (Fig. 4(c)). We noticed that, with and without flows, particles behave nearly identically at short time scales, in particular on time scales less than 100 ms. At longer time scales, however, we found that the MSD plateaus

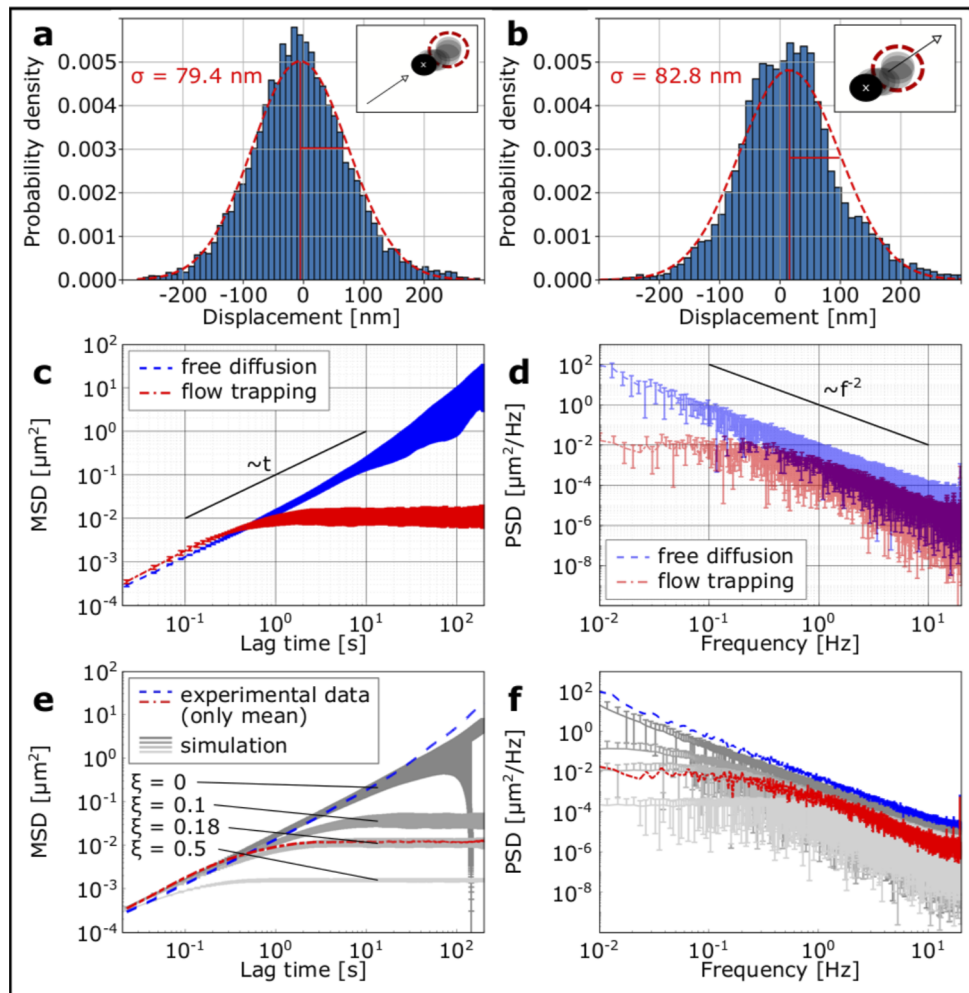


Fig. 4. Continuous re-positioning of a particle leads to suppression of random diffusive motion. a) and b) Histogram of particle distance to target position along the x-coordinate for a flow field pushing and pulling, respectively, on the particle (see also [Visualization 4](#) and [Visualization 5](#), respectively). In both cases, the particle was held in place for 5 min. c) and d) Mean squared displacement (MSD) and power spectral density (PSD) of a diffusive particle vs. a particle kept in position by the feedback-controlled flow fields. e) and f) Results of simulations compared to experimental results: MSD and PSD, respectively. In the simulations, ξ denotes the correction efficiency, the ratio between the diffusive step size and the step size of the motion back to the target, created by the feedback loop application of thermoviscous flows.

at a finite value around $0.01 \mu\text{m}^2$ in the presence of re-positioning flows, whereas the MSD keeps on growing linearly in the absence of flows. This analysis shows that a confinement inferred from the histogram analysis of particle position is based on the suppressed diffusive motion at long time scales, while still permitting diffusion displacements at short time scales.

As this behavior is similar to that observed in optical tweezers, we asked if we could also observe the characteristics of reduced motion at low frequencies and potentially a corner frequency in the power spectral density (PSD) of the particle trajectories. For the calculation of the MSD and PSD MATLAB algorithms from Stoev *et al.* were used [26]. We indeed found a plateau for frequencies up to 0.4 Hz in the PSD of a confined particle. For higher frequencies the PSD declined, showing a slope proportional to the frequency to the power of -2 and overlapping with the PSD of a diffusing particle. Furthermore, we found that simple simulations of a diffusing particle that is exposed to a constant velocity bias towards a target for a theoretically calculated diffusion coefficient of $0.008 \mu\text{m}^2/\text{s}$ (at 20 °C, see Supplement 1) are sufficient to reproduce these results (Fig. 4(e) and (f)). This concerns the plateaus in the MSD and PSD plot at long time scales and low frequencies, respectively, but also the slightly reduced power spectrum at high frequencies for trapped particles. The latter point shows that reduced motion at higher frequencies is not an experimental artifact stemming from unknown physical contributions. These simulations emphasize that our understanding of the underlying physics is sufficient to explain the experimentally observed emergent behavior of particle confinement and the attenuation of its translational power spectrum.

3. Discussion

Here, we have described proof of principle experiments and their physical analysis showing that optically induced thermoviscous flows can be utilized in a feedback-controlled manner to achieve high-precision positioning of single colloidal particles, without the need for optical forces [2] and free from related material constraints. As we have shown, the effect is due to hydrodynamic repositioning rather than optical trapping or thermophoresis. The positioning precision of up to 24 nm is about 3 times greater than the highest precision reported based on classic, pump-based microfluidics [17]. As the exploited thermoviscous flows do not depend on the absolute viscosity of the medium, this precision can likely still be increased in a medium of higher viscosity, where diffusion dynamics are further reduced.

Due to the spatial confinement of the flow fields and their $1/r^2$ decay in the far-field, we see particular advantages when expanding the method towards the multiplexed positioning of beads (see outlook). Our experiments also demonstrate that, in contrast to optical trapping, a particle can be positioned without exposing the particle to the laser beam, which might be advantageous when photodamage of sensitive particles (such as biological compartments or protein condensates) is a concern. Furthermore, hydrodynamic positioning does not require particles with a high refractive index.

As observed with optical trapping, the reduced diffusion goes along with a reduction of the PSD. Although in optical trapping the existence of a corner frequency, below which the PSD plateaus, can be used to calculate a spring constant for the repositioning of trapped particles within a parabolic trapping potential, this analogy is likely only phenomenological. While beyond the scope of this paper, we would not expect a linear force-displacement relation, as the currently employed feedback algorithm renders flow velocities around the particle independent of the particle's distance from its destination. Nevertheless, using alternative flow fields might also allow thermoviscous flow fields to be used for force sensing. Given that frictional forces are known to be very weak at the typical velocities that we introduce, this could result in highly sensitive force measurements.

4. Conclusion and outlook

We have shown that by employing a closed feedback loop, micron-size colloidal particles can be position controlled with subdiffraction precision using optically controlled thermoviscous flows. As our method to position particles shows high versatility, low restrictions on particle materials, and may leverage advanced optical technologies to drive flow fields using dynamic laser patterns, we see a wide range of applications emerging which will motivate further developments.

4.1. *Multiplexed particle positioning*

With the ability to move a single particle, the next logical question will be if multiple particles can be moved with respect to each other in a controlled manner. Here, the spatial confinement of optically generated flow fields and their $1/r^2$ scaling might enable the simultaneous positioning of increased numbers of particles compared to classic microfluids. Spatial control of particle positioning would be useful for the delivery of single particles to cells, the assembly of cells for on-chip physico-chemical analysis [27] or the assembly of colloidal structures at defined stoichiometry. Furthermore, this could complement 3D additive lithography [28], the assembly of cell colonies as well-defined starting points for organoid and tissue growth and delivery of tissue fragments into microfluidic channels for on-chip sequencing. Important in this development will be the ability to generate flow fields that position particles in parallel while avoiding displacement of already positioned particles. So far, the presented manipulations were carried out in an effective 2D geometry. In the future, it would be interesting to see if depth-discriminative dynamic heating strategies could be used to control particle position also in the third dimension. Once multiple particles can be brought to their respective positions in parallel, it might be feasible to update their target positions continuously and thereby transition from spatial assembly to a dynamic assembly that could be used to drive micron-scale machines and robots. Key here will be advanced control strategies to find experimentally feasible laser scan paths or otherwise dynamic laser fields that give rise to flows that guide the particles close to their time-dependent destinations. Towards this end we see potential in both evolutionary algorithms and reinforcement learning strategies.

4.2. *Force-sensitive positioning*

By comparing the actual positions of particles to their expected positions, it might be possible to infer forces acting on the particles. Given that flow-induced forces are typically weak, such force sensing might be particularly sensitive. For some applications, it might be beneficial to be able to control particles interactively via hand gestures, for which mixed reality devices offer an attractive and likely compatible solution. Force feedback interfaces could enable tactile interactive manipulations.

4.3. *In-vivo manipulations*

Precision manipulation within the interior of cells and embryos might also depend on numerical models that take into account spatial heterogeneities in the sample. These could be rigid walls, such as the egg shell of an embryo, or spatial changes in the visco-elastic properties of the cell and nucleoplasm. Applications of the positioning of particles in cells and embryos include the non-invasive induction of medically relevant phenotypes, such as chromosome mis-segregations, the inference of structure function relationships, or the positioning of developmental cues, such as centrosomes [29].

Acknowledgements. E. Erben & M. Kreysing conceived the experiments. E. Erben and N. Maghelli carried out the experiments and collected data. N. Maghelli and S. Klykov developed control software. B. Seelbinder carried out and analyzed the experiments on flow field characterization. E. Erben analyzed the particle position data. I. Stoev carried out the MSD and PSD analysis of the particle position data. E. Erben conducted the simulations. M. Kreysing supervised the research. E. Erben and M. Kreysing wrote the manuscript. All authors read the manuscript and participated in critical discussions of the research.

Disclosures. E. Erben, M. Kreysing and N. Maghelli apply for a European patent for technology related to this publication. M. Kreysing declares an ongoing consultancy relationship with Rapp Optoelectronic GmbH.

Data availability. Data underlying the results presented in this paper are not publicly available at this time but may be obtained from the authors upon reasonable request.

Supplemental document. See [Supplement 1](#) for supporting content.

References

1. A. Ashkin, J. M. Dziedzic, J. E. Bjorkholm, and S. Chu, "Observation of a single-beam gradient force optical trap for dielectric particles," *Opt. Lett.* **11**(5), 288–290 (1986).
2. A. E. Wallin, H. Ojala, E. Hægström, and R. Tuma, "Stiffer optical tweezers through real-time feedback control," *Appl. Phys. Lett.* **92**(22), 224104 (2008).
3. M. J. Guffey and N. F. Scherer, "All-Optical Patterning of Au Nanoparticles on Surfaces Using Optical Traps," *Nano Lett.* **10**, 4302–4308 (2010).
4. P. Polimeno, A. Magazzù, M. A. Iatì, F. Patti, R. Saija, C. D. Esposti Boschi, M. G. Donato, P. G. Gucciardi, P. H. Jones, G. Volpe, and O. M. Maragò, "Optical tweezers and their applications," *J. Quant. Spectrosc. Radiat. Transfer* **218**, 131–150 (2018).
5. T. R. Strick, J.-F. Allemand, D. Bensimon, A. Bensimon, and V. Croquette, "The Elasticity of a Single Supercoiled DNA Molecule," *Science* **271**(5257), 1835–1837 (1996).
6. C. Gosse and V. Croquette, "Magnetic Tweezers: Micromanipulation and Force Measurement at the Molecular Level," *Biophys. J.* **82**(6), 3314–3329 (2002).
7. R. Sarkar and V. V. Rybenkov, "A Guide to Magnetic Tweezers and Their Applications," *Front. Phys.* **4**, 48 (2016).
8. A. E. Cohen and W. E. Moerner, "Method for trapping and manipulating nanoscale objects in solution," *Appl. Phys. Lett.* **86**(9), 093109 (2005).
9. M. D. Armani, S. V. Chaudhary, R. Probst, and B. Shapiro, "Using feedback control of microflows to independently steer multiple particles," *J. Microelectromech. Syst.* **15**(4), 945–956 (2006).
10. H. M. Hertz, "Standing-wave acoustic trap for noninvasive positioning of microparticles," *J. Appl. Phys.* **78**(8), 4845–4849 (1995).
11. M. Fränzl, T. Thalheim, J. Adler, D. Huster, J. Posseckardt, M. Mertig, and F. Cichos, "Thermophoretic trap for single amyloid fibril and protein aggregation studies," *Nat. Methods* **16**(7), 611–614 (2019).
12. J. Zhang, B. A. Grzybowski, and S. Granick, "Janus Particle Synthesis, Assembly, and Application," *Langmuir* **33**(28), 6964–6977 (2017).
13. A. T. Ohta, A. Jamshidi, J. K. Valley, H.-Y. Hsu, and M. C. Wu, "Optically actuated thermocapillary movement of gas bubbles on an absorbing substrate," *Appl. Phys. Lett.* **91**(7), 074103 (2007).
14. D. D. Carlo, L. Y. Wu, and L. P. Lee, "Dynamic single cell culture array," *Lab Chip* **6**(11), 1445–1449 (2006).
15. Q. Luan, C. Macaraniag, J. Zhou, and I. Papautsky, "Microfluidic systems for hydrodynamic trapping of cells and clusters," *Biomicrofluidics* **14**(3), 031502 (2020).
16. M. Tanyeri, E. M. Johnson-Chavarría, and C. M. Schroeder, "Hydrodynamic trap for single particles and cells," *Appl. Phys. Lett.* **96**(22), 224101 (2010).
17. A. Shenoy, C. V. Rao, and C. M. Schroeder, "Stokes trap for multiplexed particle manipulation and assembly using fluidics," *Proc. Natl. Acad. Sci. U. S. A.* **113**(15), 3976–3981 (2016).
18. C. M. Lin, Y. S. Lai, H. P. Liu, C. Y. Chen, and A. M. Wo, "Trapping of Bioparticles via Microvortices in a Microfluidic Device for Bioassay Applications," *Anal. Chem.* **80**(23), 8937–8945 (2008).
19. B. R. Lutz, J. Chen, and D. T. Schwartz, "Hydrodynamic Tweezers: 1. Noncontact Trapping of Single Cells Using Steady Streaming Microeddies," *Anal. Chem.* **78**(15), 5429–5435 (2006).
20. D. Kumar, A. Shenoy, J. Deutsch, and C. M. Schroeder, "Automation and flow control for particle manipulation," *Curr. Opin. Chem. Eng.* **29**, 1–8 (2020).
21. F. M. Weinert, J. A. Kraus, T. Franosch, and D. Braun, "Microscale Fluid Flow Induced by Thermoviscous Expansion Along a Traveling Wave," *Phys. Rev. Lett.* **100**, 164501 (2008).
22. F. M. Weinert and D. Braun, "Optically driven fluid flow along arbitrary microscale patterns using thermoviscous expansion," *J. Appl. Phys.* **104**(10), 104701 (2008).
23. M. Mittasch, P. Gross, M. Nestler, A. W. Fritsch, C. Iserman, M. Kar, M. Munder, A. Voigt, S. Alberti, S. W. Grill, and M. Kreysing, "Non-invasive perturbations of intracellular flow reveal physical principles of cell organization," *Nat. Cell Biol.* **20**(3), 344–351 (2018).
24. M. Mittasch, V. M. Tran, M. U. Rios, A. W. Fritsch, S. J. Enos, B. Ferreira Gomes, A. Bond, M. Kreysing, and J. B. Woodruff, "Regulated changes in material properties underlie centrosome disassembly during mitotic exit," *J. Cell Biol.* **219**(4), 36 (2020).
25. N. T. Chartier, A. Mukherjee, J. Pfanzelter, S. Fürthauer, B. T. Larson, A. W. Fritsch, M. Kreysing, F. Jülicher, and S. W. Grill, "A hydraulic instability drives the cell death decision in the nematode germline," *bioRxiv* 2020.05.30.125864 (2020).
26. I. D. Stoev, A. Caciagli, Z. Xing, and E. Eiser, "Using single-beam optical tweezers for the passive microrheology of complex fluids," in *Optical Trapping and Optical Micromanipulation XV* (International Society for Optics and Photonics, 2018), Vol. 10723, p. 107232D.

27. M. Hippler, E. D. Lemma, S. Bertels, E. Blasco, C. Barner-Kowollik, M. Wegener, and M. Bastmeyer, "3D Scaffolds to Study Basic Cell Biology," *Adv. Mater.* **31**(26), 1808110 (2019).
28. M. Deubel, G. von Freymann, M. Wegener, S. Pereira, K. Busch, and C. M. Soukoulis, "Direct laser writing of three-dimensional photonic-crystal templates for telecommunications," *Nat. Mater.* **3**(7), 444–447 (2004).
29. M. Kreysing, "Probing the Functional Role of Physical Motion in Development," *Dev. Cell* **51**(2), 135–144 (2019).